



**HAL**  
open science

# NUMERICAL SIMULATION OF WAVE PROPAGATION IN HETEROGENEOUS AND RANDOM MEDIA FOR SITE EFFECTS ASSESSMENT IN THE GRENOBLE VALLEY

Emmanuel Chaljub, Malcon Celorio, Cécile Cornou, Florent de Martin, Elias El  
Haber, Ludovic Margerin, Jules Marti, Irmela Zentner

## ► To cite this version:

Emmanuel Chaljub, Malcon Celorio, Cécile Cornou, Florent de Martin, Elias El Haber, et al.. NUMERICAL SIMULATION OF WAVE PROPAGATION IN HETEROGENEOUS AND RANDOM MEDIA FOR SITE EFFECTS ASSESSMENT IN THE GRENOBLE VALLEY. Sixth IASPEI/IAEE International Symposium on the Effects of Surface Geology on Seismic Motion, Aug 2021, Kyoto (Japan), Japan. <hal-04991958>

**HAL Id: hal-04991958**

**<https://hal.science/hal-04991958v1>**

Submitted on 14 Mar 2025

**HAL** is a multi-disciplinary open access archive for the deposit and dissemination of scientific research documents, whether they are published or not. The documents may come from teaching and research institutions in France or abroad, or from public or private research centers.

L'archive ouverte pluridisciplinaire **HAL**, est destinée au dépôt et à la diffusion de documents scientifiques de niveau recherche, publiés ou non, émanant des établissements d'enseignement et de recherche français ou étrangers, des laboratoires publics ou privés.



HAL Authorization

# NUMERICAL SIMULATION OF WAVE PROPAGATION IN HETEROGENEOUS AND RANDOM MEDIA FOR SITE EFFECTS ASSESSMENT IN THE GRENOBLE VALLEY

Emmanuel Chaljub<sup>1</sup>, Malcon Celorio<sup>2</sup>, Cécile Cornou<sup>3</sup>, Florent De Martin<sup>4</sup>,  
Elias El Haber<sup>5</sup>, Ludovic Margerin<sup>6</sup>, Jules Marti<sup>7</sup> and Irmela Zentner<sup>8</sup>.

1 Researcher, Univ. Grenoble Alpes, Univ. Savoie Mont Blanc, CNRS, IRD, Univ. Gustave Eiffel, ISTerre,  
38000 Grenoble, France, (emmanuel.chaljub@univ-grenoble-alpes.fr)

2 PhD student, Univ. Grenoble Alpes, Univ. Savoie Mont Blanc, CNRS, IRD, Univ. Gustave Eiffel, ISTerre,  
38000 Grenoble, France, (malcon-humberto.celorio-murillo@univ-grenoble-alpes.fr)

3 Research Director, Univ. Grenoble Alpes, Univ. Savoie Mont Blanc, CNRS, IRD, Univ. Gustave Eiffel,  
ISTerre, 38000 Grenoble, France, (cecile.cornou@univ-grenoble-alpes.fr)

4 Researcher, BRGM (French geological survey), Orléans, France, (F.DeMartin@brgm.fr)

5 Post-doc fellow, Univ. Grenoble Alpes, Univ. Savoie Mont Blanc, CNRS, IRD, Univ. Gustave Eiffel, ISTerre,  
38000 Grenoble, France (elias.el-haber@univ-grenoble-alpes.fr)

6 Research Director, IRAP, OMP, Univ. Paul Sabatier, CNRS, CNES, Toulouse, France  
(ludovic.margerin@irap.omp.eu)

7 Master student, ISAE-SUPAERO, Toulouse, France (jules.marti@student.isae-supaero.fr)

8 EDF Lab Paris-Saclay, Palaiseau, France (irmela.zentner@edf.fr)

## ABSTRACT

During the 3<sup>rd</sup> ESG symposium held in Grenoble in 2006, the Grenoble valley was the target of a verification exercise of physics-based methods for ground motion prediction including site effects. Back then, knowledge of the velocity model was limited to large depths and prevented the application of 3D numerical simulation for frequencies higher than 1 – 2 Hz. Here we present the progress made in the design of a 3D heterogeneous model of the shallow subsurface, which combines deterministic and stochastic descriptions and we present some preliminary results of 3D numerical simulations of the seismic response of the valley performed for frequencies up to 5 Hz.

*Keywords: Numerical simulation, site effects, small-scale heterogeneities, random media, scattering attenuation.*

## INTRODUCTION

Physics-based estimation of earthquake ground motions (EGM) in the frequency range of engineering interest (from tenths to tens of Hz) requires the knowledge of the propagation medium from source to site at a spatial resolution which is currently out of reach. However, the state of practice is expected to evolve thanks to the accumulation and the dissemination of geophysical and geotechnical information, in particular in urban areas, and to the development of dense array analyses driven by either low-cost instruments or new technology such as Distributed Acoustic Sensing. These anticipated advances will improve the design of realistic deterministic propagation models and will both push forward the spatial frequency at which a stochastic description is needed and provide constraints on the random media properties (see e.g. Pitarka & Mellors, 2021). This is key to gain physical insight into the processes that control EGM and their variability (for example through the occurrence of site effects), and to develop realistic models for site-specific EGM prediction with quantified uncertainty.

Here, we report some progress and recent developments in physics-based estimation of EGM in the Grenoble valley, 15 years after the site was chosen to define a numerical benchmark for site effects evaluation at the third international ESG symposium held in Grenoble (ESG3, 2006). First, we explain how the large amount of geological, geotechnical and geophysical information gathered in the Grenoble area for decades is being analyzed to build a consistent velocity model of the subsurface. We

present a two-scale approach combining a deterministic, geology-driven macroscopic zoning and a stochastic representation of small-scale fluctuations relying mostly on the information provided by geotechnical boreholes. Then, a verification example for the simulation of seismic waves in 2D random media is shown, where we successfully compare the scattering attenuation measured on synthetics with theoretical predictions. Finally, we present some preliminary results of 3D simulation of EGM up to 5 Hz in the Grenoble valley, where the propagation medium includes a fully heterogeneous description of the shallow subsurface, in a limited area of 3 km<sup>2</sup> located in the Western part of the valley. In particular we illustrate how the different scales of heterogeneity contribute to shape ground motions, in terms of amplitude and duration, when the valley is excited by a local earthquake as recorded in the past.

### GRENOBLE VALLEY MODEL FROM ESG3 TO ESG6

The city of Grenoble is located in a Y-shaped embanked alpine valley sited on hundreds of meters of post-glacial lacustrine deposits (Figure 1a), prone to site effects (see e.g. Lebrun et al., 2001; Guéguen et al., 2007). Within the two glacial cycles involved in the formation of the Grenoble's basin, the erosive phase was followed by the installation of a lake that was then infilled with fine homogeneous sediments (sandy or clayey silts). These lake deposits were finally covered with heterogeneous alluviums coming from 2 rivers, which are the Drac river, coming from the South, and the Isère river, coming from the North East (Figure 1b). Being a highly energetic river, the Drac river has caused several large floods in the past covering the entire part of the Grenoble's valley up to the Isère river in the North (Lacroix, 1971) and its bed was diverted to the West, close to the Vercors massif. The numerical model used for the ESG3 benchmark (see Chaljub et al., 2010, and references therein) was built by combining bedrock topography inferred from gravimetric data (Vallon, 1999) and seismic velocities obtained from a 6 km long seismic refraction profile in the Western part of the valley and from down-hole seismic measurements at the deep borehole site of Montbonnot in the Eastern Grésivaudan valley (Cornou, 2002). This laterally homogeneous model still satisfactorily represents the state of geological and geophysical knowledge of the deep basin.

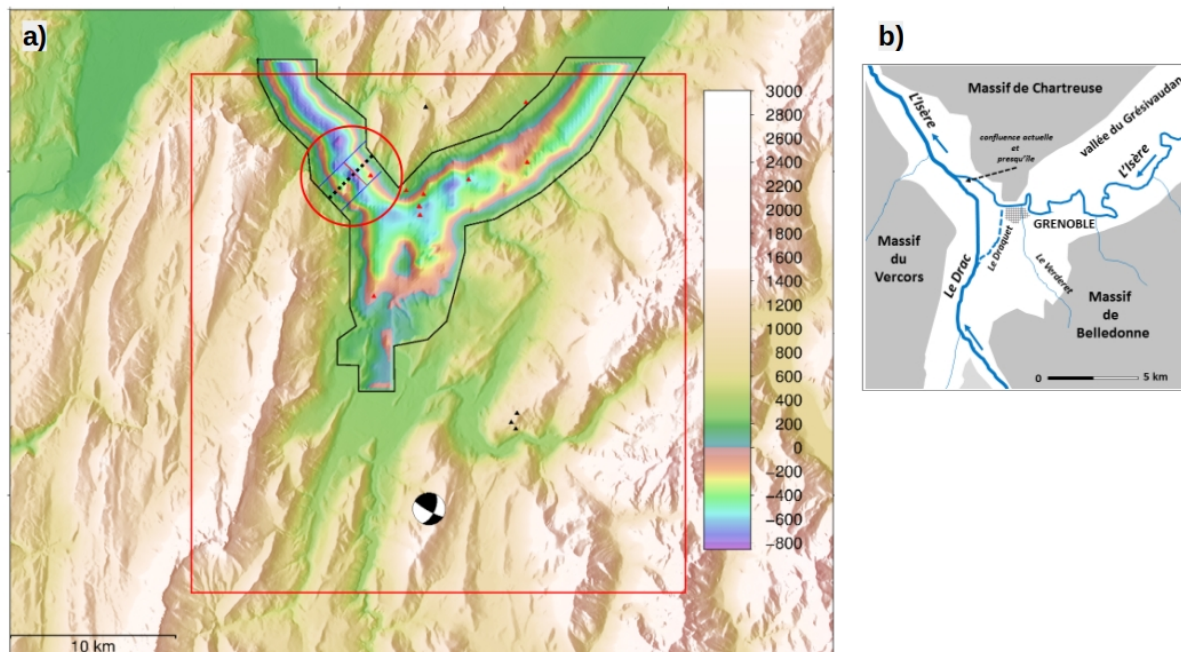


Figure 1: a) Surface and bedrock elevation maps in the Grenoble area. Color indicates elevation (in m) wrt sea level. The red circle (and the rectangle inside delimited by blue lines) in the Western part shows the area around ILL, which is the focus of the EXAMIN project (see text). Black dots indicate the location of a 2D profile where simulations results are presented and the beachball is located at the epicenter of the 1999 Laffrey event. b) Schematic view of the actual location of the Drac and Isère rivers (After Dumas & Favillier, 2017).

In order to improve the model of the first  $\sim 100$  m of heterogeneous sediments resulting from the dynamics of river deposits, a series of geophysical measurements have been conducted since 2003 to characterize shear-wave velocities (Tadunema, 2003; Tsuno et al., 2008; Bard, Cornou and Wathelet, 2010; Rivanedeira, 2012; Grandjean, 2013; Garofalo et al., 2016; Hollender et al., 2017). These measurements included active surface waves measurements (MASW) performed at 110 different sites (Figure 2a) and passive surface wave measurements at 15 arrays (Figure 2a).

Although large, the number of geophysical measurements is still not sufficient to enable fine spatial imaging of the shear-wave structure in the near-surface. Information from geological and geotechnical boreholes (with depth ranging from 10 m to about 40 m) were thus collected at 1350 locations (see Cartier and Cornou, 2016, and Figure 2a). Comparison of shear wave velocities derived from surface wave measurements, with surface geology at the center of the basin (Collombet, 2009, zone B in Figure 2b), Northwestern branch of the basin (Rivaneidera, 2012, zone A in Figure 2b) and Eastern part of Grenoble (Grandjean, 2013, zone C in Figure 2b) reveals very consistent relationship between the surface geological units (gravels, sands, clays) and the related shear-wave velocity, whatever the site location. High values of shear-wave velocities (350-400 m/s) correspond to coarse sediment deposits (sands, gravels) from the Drac river in the Western part of the basin, while lower values (100-250 m/s) correspond to the fine grained deposits from the Isère river in the Eastern part of Grenoble and the Grésivaudan valley.

In order to get a fine spatial resolution of the velocity structure, shear-wave velocity values were attributed to the various geological units using the relationships between geological units and mean shear-wave velocities: clay, backfill, sand and gravel units were thus attributed shear-wave velocities of 150 m/s, 250 m/s, 400 m/s and 400 m/s, respectively. Shear-wave velocity models from the surface to the borehole depth were then estimated, assuming a P-wave velocity of 1500 m/s and bulk density of  $1800 \text{ kg/m}^3$ . Distribution of theoretical fundamental Rayleigh wave phase velocities computed from these velocity models and experimental phase velocities derived from geophysical measurements at 10 m wavelength are displayed in Figure 2b. The phase velocity map indicates sharp East-West lateral variations of near-surface shear-wave velocities in relation with the dynamics of the fluvial deposits of the Drac and Isère rivers.

Within the framework of the EXAMIN project, statistical variability properties of the small-scale shear-wave velocity heterogeneities have been derived in the Northwestern branch of the basin (Figure 3b), in the area of the Lau Langevin Institute (hereafter referred to as ILL), a reactor-based facility which provides the most intense neutron source in the world. The ILL area exhibits a strong lateral variation of the shallow deposits, dominated by clays in the Southwestern part (left bank of the Isère river) and clays and gravels in the Northeastern part (right bank). Using shear-wave velocity profiles from the surface to 20 m depth inferred from geological boreholes, coefficient of variation (COV) of shear-wave velocity was computed at each borehole location provided that at least 10 boreholes were located within 200 m of the target borehole. Correlation distances, that quantify the spatial fluctuations of  $V_s$  along the vertical and horizontal directions, were also computed considering exponential decaying auto-correlation function as implemented in the DACE kriging matlab toolbox (Søndergaard et al., 2002). Consistently with a coefficient of variations of  $V_s$  being slightly larger in the Western zone of the studied area (mean of 40 +/- 4%) compared to the Eastern zone (mean of 30 +/- 11%) (Figure 3a), horizontal correlation distances exhibit lower values in the Western zone compared to the Eastern one, mean horizontal correlation distances including both zones being about 20 m +/- 5%.

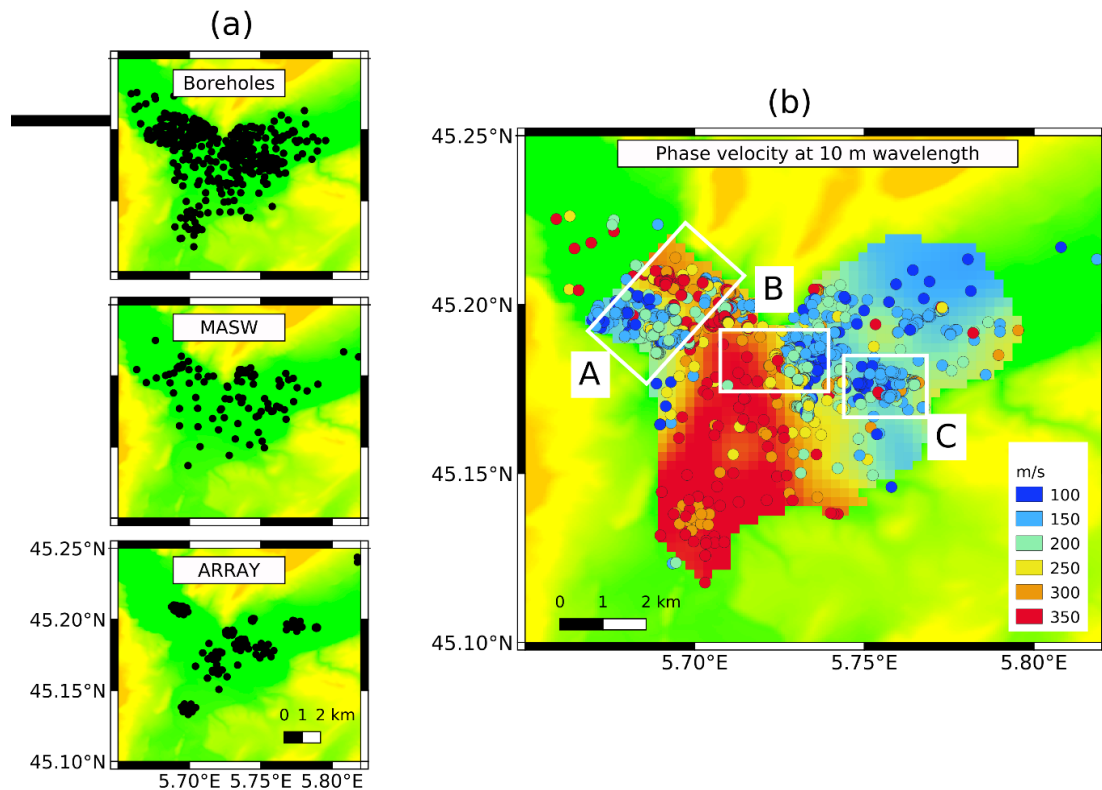


Figure 2: (a) Location of geological boreholes (boreholes) and geophysical (active, MASW, and passive surface waves, ARRAY) measurements. (b) Spatial distribution of fundamental Rayleigh wave phase velocities (colored filled circles) at 10 m wavelength and interpolated map. White rectangles indicate boreholes investigated by A: Rivanedeira (2012), B: Collombet (2009) and C: Grandjean (2013).

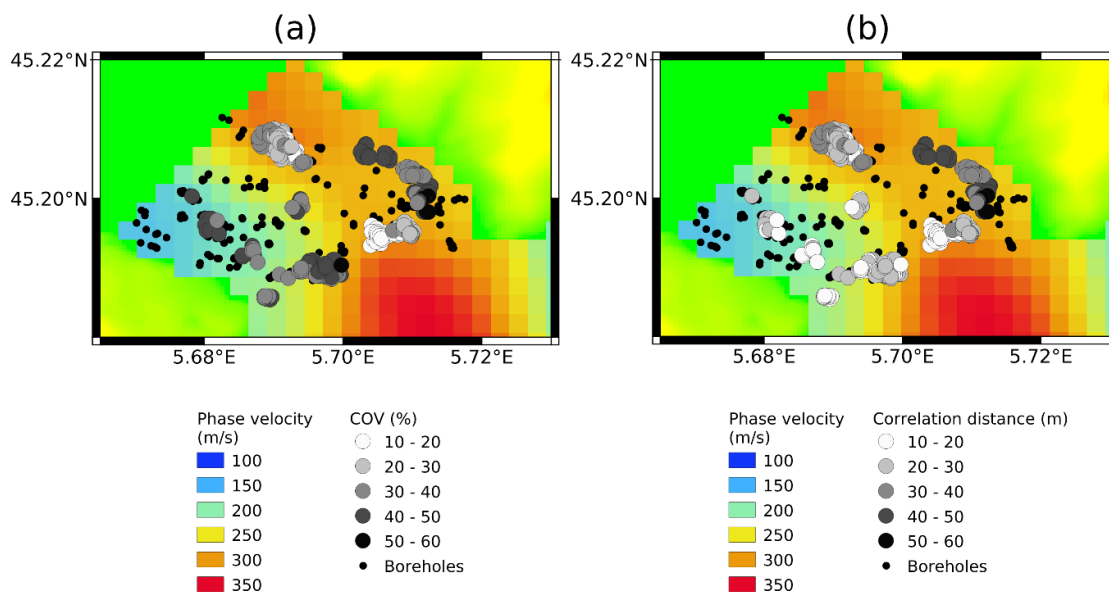


Figure 3: (a) Coefficient of variation of  $V_s$  from surface to 20 m depth and (b) horizontal correlation distance of  $V_s$  from surface to 20 m depth overlaying the phase velocity map at 10 m wavelength. Boreholes location are indicated by black dots.

## SIMULATION OF SEISMIC WAVES IN HETEROGENEOUS AND RANDOM MEDIA

Numerical simulation of seismic waves radiation and propagation in 3D heterogeneous media for EGM prediction is a subject of active research (see e.g. Moczo et al., 2021 in the current ESG6 proceedings) and gradually enters current practice in site-specific seismic hazard assessment. In order to achieve an acceptable degree of realism, it is necessary to be able to represent the small-scale heterogeneity that affects the radiation and propagation of the minimum wavelength considered. Given the frequency range relevant to engineering applications and the presence of low velocity sediments, minimum propagated wavelengths are generally at least around tens of meters, implying that their description cannot be fully deterministic.

The inclusion of random fluctuations in seismic wave velocity and density is common in crustal studies, particularly for modeling coda waves propagation (see e.g. Sato et al., 2012 and references therein). Their effect on strong ground motion has been considered more recently in EGM prediction (see e.g. Hartzell et al. 2010; Imperatori & Mai, 2012; Iwaki et al., 2018; Withers et al. 2018; Pitarka & Mellors, 2021). This can be understood partly because of the late availability of computational resources needed for direct numerical simulation of EGM at high frequency but also because the properties of random media for the shallow subsurface are different from those of the deep crust (stronger contrasts exist and more complex auto-correlation functions are expected).

Interestingly, the implementation of random media in numerical codes and the verification of the numerical solutions obtained is often overlooked, whereas it is not a simple matter. We refer to Liu et al. (2019) for a review of existing methods and codes for the realization of random media and to Przybilla et al. (2006) and Emoto & Sato (2018) for examples of careful comparisons of coda envelopes simulated by the finite difference method in 2D and 3D elastic media with predictions obtained with the radiative transfer theory. In what follows, we propose a 2D verification example based upon the properties of the coherent wavefield to ensure that the scattering attenuation is well simulated. Next we present 3D simulations of EGM in the 3D heterogeneous model introduced in the previous section.

### Verification on a Simple 2D Example

We consider the simplest possible example of a 2D homogeneous background elastic medium with shear wave velocity  $V_0=3.14$  km/s and density  $\rho_0=2500$  kg/m<sup>3</sup>, on which zero-mean fluctuations are superimposed. The velocity fluctuations are correlated with those of density through

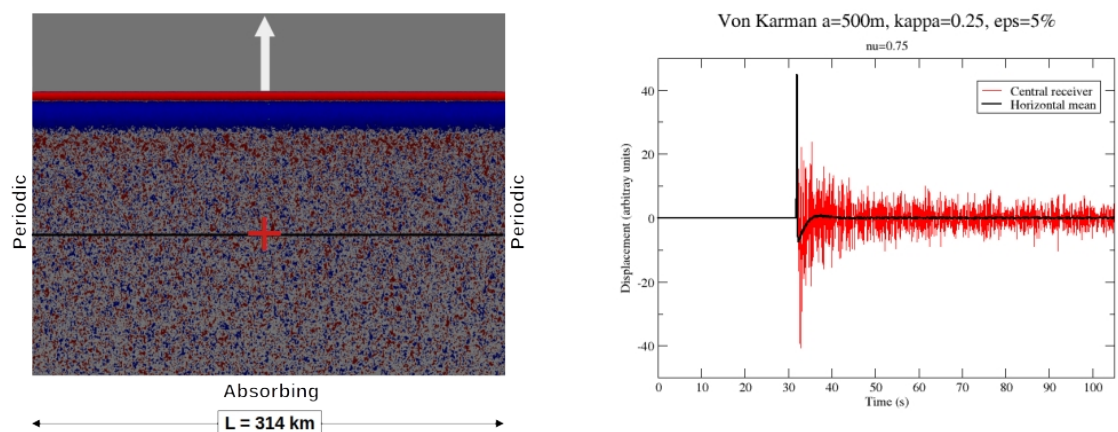


Figure 4: **Left:** snapshot of 2D SH plane wave propagating vertically (upward) in a random medium having a von Karman auto-correlation function (the heterogeneities are not shown). Red/blue colors stand for positive/negative displacement. **Right:** displacement (red) recorded at a central receiver (red cross in the left figure) after 100 km of propagation and mean displacement (black) obtained by averaging along the horizontal black line of the left figure.

$dV/V_0 = \nu d\rho/\rho_0$ , where  $\nu$  typically varies between 0 and 1. The fluctuations are defined through their auto-correlation function (ACF), which is of von Karman type, with typical crustal values: correlation length  $a=500$  m, Hurst exponent  $\kappa=0.25$  and standard deviation  $\varepsilon=5\%$ . The medium is excited by a vertically incident plane wave as shown in Figure 4. The computational domain is a square of size  $L=314$  km, with periodic vertical boundaries and absorbing horizontal boundaries.

The domain is meshed with  $10^6$  squared elements of size  $Le=314$  m and a polynomial order  $N=4$  is used inside each element to build a spectral element solution of the wave equation in the elastic domain (no intrinsic attenuation is assumed). The interaction of a given seismic wavelength  $\lambda$  with the random medium requires all heterogeneities with size larger than  $\lambda/2$  to be well discretized. The 2D spectral element grid allows to represent fluctuations of size  $Le/2$ , with about 2.5 points per spatial wavelength, and to simulate accurately the propagation of seismic wavelengths over large distances (up to 100 wavelengths) for wavelengths above a minimum size between  $2*Le$  (with 10 points per  $\lambda$ ) and  $Le$  (with 5 points per  $\lambda$ ). In terms of normalized wavenumbers,  $ka$ , our choice of the background velocity yields  $ka=f$ , with  $f$  the frequency. We consider that the propagation of seismic waves in such random medium is accurately simulated at least in the range  $ka \leq 5$ .

Time series of the displacement recorded after 100 km of propagation is shown in Figure 4 (red curve) for a random medium in which the correlation between velocity and density fluctuations is  $\nu=0.75$ . The source time function is a Dirac pulse, which has been low-pass filtered below 8 Hz to yield negligible energy for frequencies higher than 10 Hz. The black curve denotes the horizontal spatial average of displacement, which is internally computed during run-time. This spatial average has been verified to correspond to the mean displacement computed from 60 realizations of the random medium, which means that the ergodicity assumption holds and that the spatial average yields the so-called coherent displacement wavefield. Properties of the coherent wavefield are used to verify the implementation of the density and velocity fluctuations and the accuracy of wave propagation in random medium. In particular, we compare the effective, here purely scattering, attenuation measured on the synthetics with theoretical predictions of the mean free path obtained by solving the Dyson equation for the coherent wavefield. The results are presented in Figure 5b for different values of the correlation coefficient  $\nu$  (0, 0.5, 1). They show that the scattering attenuation is well reproduced in the synthetics.

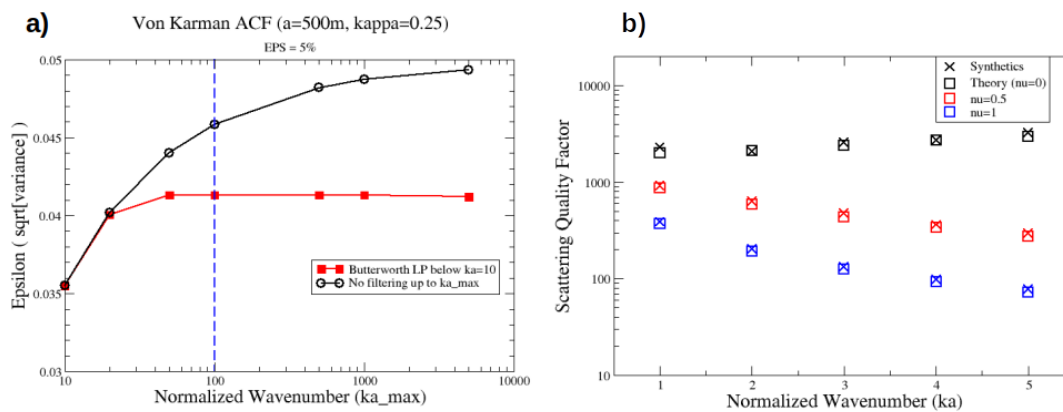


Figure 5: a) Effect of truncating the spectral representation of the ACF in Fourier space on the standard deviation of the fluctuations. b) Comparison of scattering quality factors measured from synthetics (crosses) with theoretical values (boxes) for different velocity-density perturbations.

The left part of the figure (Figure 5a) shows the evolution of the standard deviation of the random medium generated at the discrete level. In our case, we synthesize the random fluctuations in the Fourier domain following Sato et al. (2012), up to a maximal normalized wavenumber  $ka_{max}=100$ , then we apply a Butterworth 4 poles low-pass filter below  $ka_c=10$ . This yields a standard deviation slightly above 4%, instead of the 5% target. Despite this bias, which is inherent to the spectral method,

we see that the scattering attenuation is well modeled, which is consistent with theory (scattering attenuation is a band-limited phenomenon in the wavenumber domain). Current work is done to compare other quantities, such as physical dispersion, which are in principle sensitive to the full wavenumber spectrum.

### 3D Simulations in the Grenoble Basin: Model and Mesh

As detailed above, the 3D Grenoble basin, which total depth reaches approximately 1 km, is composed of a main layer of post-glacial lacustrine sediments overlaid by a few tens of meters of alluvial deposits (clays, sands, gravels), the geometry and composition of which result from the complex activity of the two rivers, Isère and Drac, over time. For the deepest part of the basin, the S-wave velocity is defined as  $V_s = 300 + 19 \cdot \sqrt{d}$ , with  $d$  being depth. It increases from about 434 m/s at 50 m depth to 855 m/s at the deepest point of the basin. This 1D S-velocity model was extended up to the surface in order to define the Grenoble basin model used during ESG3 (Chaljub et al., 2010). To account for the shallower part of the sedimentary filling in the ILL area, the uppermost 50 m layer is split (along a non-vertical boundary) into a clay zone in the Southwestern part of the valley and a gravel zone in the Northeast. The surface imprint of the heterogeneous area covers the whole valley (from edge to edge) and is about 1 km wide. It corresponds to the area delimited by blue lines in Figure 1a. The mechanical properties within the ILL area are first assumed to be constant in each zone, for example  $V_s$  is 250 m/s for the clay and 375 m/s for the gravel, respectively. The other properties, including density and P-wave velocities are summarized in Table 1. Random, zero-mean fluctuations are further superimposed on the background S- and P- velocities in each zone, assuming an exponential ACF (that is, a von Karman ACF with Hurst exponent  $\kappa = 0.5$ ) with 50 m, 100 m and 200 m correlation lengths ( $L_c$ ) and a 5% standard deviation ( $\varepsilon$ ). This choice of such rather small COV was a compromise between the target maximum frequency (5 Hz) and the computational resources available for the project, as smaller values of  $V_s$  would lead to larger meshes and smaller time steps which have to be dealt with for each realization of the random fluctuations.

Table 1: Mechanical properties of the Grenoble multi-layer sedimentary basin including random fluctuations in the ILL heterogeneous area.

Layer	Hmax	$\rho$	$V_s$	$V_p$	$Q_s$	$Q_p$	$L_c$	$\varepsilon$	PDF
	m	kg/m <sup>3</sup>	m/s	m/s	–	–	m	–	–
Gravel	50	2140	375	1450	50	50	50-200	0.05	exp
Clay	50	1700	250	1200	50	50	50-200	0.05	exp
Lacustrine Sediments	855	2140-2246	300-855	1450-2476	50	800	–	–	–
Bedrock1	6175	2720	3200	5600	5000	5000	–	–	–
Bedrock2	–	2720	3430	5920	5000	5000	–	–	–

The heterogeneities are modeled in the spatial domain by a Karhunen-Loève (KL) approximation (e.g., Karhunen 1947; Loève 1968) which relies on the computation of the eigenmodes of the Fredholm integral equation associated with the (here exponential) covariance kernel. The solutions are searched on the interval [0:1] using a normalized correlation length. This allows dealing with normalized solutions for which general error bounds can be evaluated once and for all. These error bounds indicate how many eigenmodes have to be retained in order to obtain the desired precision. For the ILL area, the number of KL modes used to generate three sets of a random field with a correlation length of 50 m, 100 m and 200 m are 76261, 20926 and 11666, respectively. In order to avoid large computational time for the random field generation due to a domain that is much larger than the correlation length, we truncated on purpose the number of eigenmodes to 70%, 80% and 90% of the optimal precision. To mitigate this issue, Panunzio et al. (2018) proposed to divide the domain into sub-domains where the modal decomposition can be locally computed.

The viscoelastic response of the sedimentary basin is computed with *efispec*, a high-performance 3-D physics-based solver (De Martin, 2011) implementing the spectral-element method in space and a second-order finite-difference method in time, as introduced in seismology by Komatitsch & Vilotte (1998). Its accuracy has been verified for site effect estimation in complex sedimentary basin configurations (Chaljub et al., 2015). The inclusion of arbitrary (excluding non-unique mapping) geological layers into the finite element unstructured hexahedral mesh – without the mesh following the geological interfaces – is done using a simple, isotropic, one-dimensional vertical homogenization method as proposed by Capdeville et al. (2010). This strategy allows us to design a mesh semi-automatically by refining the surface imprint of the valley down to a constant given depth (here 1000 m) in order to include the whole basin as shown in Figure 6a. The mesh used for simulation up to 5 Hz is composed of 2 965 154 hexahedral elements of approximately three sizes: 450 m, 150 m and 50 m and a polynomial order  $N=4$  is used in each element. The generation of the random fields filling the clay and gravel geological layers is made by first performing the KL expansion, then the vertical homogenization. The resulting S-velocity field in the ILL target area is shown in Figure 6b.

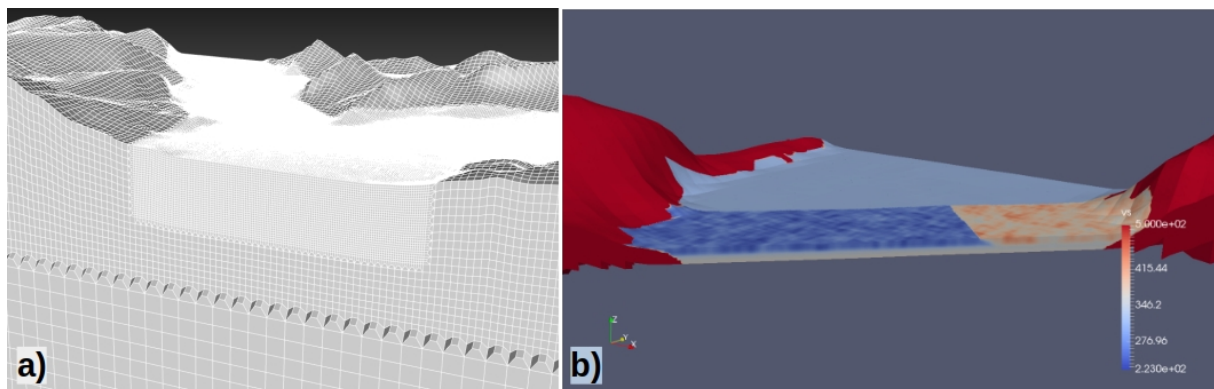


Figure 6: a) view from the Southeast of the spectral element mesh used for simulation of the seismic response of the Grenoble basin for frequencies up to 5 Hz. b) zoom on the shear wave velocity fluctuations in the ILL area superimposed on a composite background model having clay and gravel zones for depth lower than 50 m.

### 3D Simulations in the Grenoble Basin: Results

The viscoelastic response of the Grenoble basin has been computed for frequencies up to 5 Hz for different seismic sources, ranging from point-sources to extended faults with imposed kinematics. Although our solver is efficiently parallelized using the Message Passing Interface (MPI), the cost of a single simulation (which requires solving 600 million equations) still amounts to 5h 30m on 1,000 cores. Here we only show the results obtained in the simplest case of a double-couple point-source representing the source of the Laffrey 1999 M3.5 event studied in Thouvenot et al. (2003). The source time function is a pseudo Heaviside which yields a flat far-field displacement spectrum, and the total duration of the simulations is 30 s. A total of 31 runs have been performed: a reference simulation with the background model, which includes the piece-wise heterogeneous subsurface model in the ILL area, and 10 realizations of each of the three random media with correlation lengths  $L_c=50, 100$  and  $200$  m (see Table 1). The East-West component of ground acceleration along a 2D  $N45^\circ$  profile (dotted black line in Figure 1a) is shown in Figure 7c for the reference simulation. The large number of receivers along the profile (441, corresponding to an inter-distance of about 7 m) allows to display the seismic wavefield without spatial aliasing. The geological cross-section along the profile, represented in Figure 7d, helps to interpret the seismic section. In particular, it is seen that the variation of the bedrock-sediment interface along the profile is quite pronounced, and that it causes a de-focusing of the direct S wave between about 1200 m and 1700 m (the arrival of the S wave can be identified around 6 s at the Southern edge, at zero offset). The transition between clay and gravel zones around 2200 m is also seen to have a strong effect on the propagation of local surface waves, in particular it reflects a significant part of the local surface wave energy generated at the Southern edge back to the Southern clay zone. Focusing effects on the vertically propagating body waves as well as interferences

with local surface waves diffracted off the valley edges participate to the high amplitudes located roughly above the local maxima of the lacustrine sediment thickness at offsets around 1000 m and 2200 m, the latter location being also close to the clay-gravel transition. Those complex effects yield large spatial variations of Arias intensity (AI) and of AI-based duration (AD) along the profile, as shown in Figure 7a and Figure 7b, respectively. AD is defined following (Trifunac & Brady, 1975) as the length of the time interval where AI reaches between 5% and 95% of its final value. Note that AI and AD appear to be roughly anti-correlated. Although not systematic, anti-correlation of amplitude (or amplification) and duration (or duration lengthening) has been reported in other studies, for example in the case where amplification is dominated by vertical propagation of S waves at resonance frequencies and duration by the Airy phases of horizontal propagation of locally diffracted surface waves (see e.g. Maufroy et al., 2017). Plotting AI as a function of AD for the reference simulation (Figure 8a) confirms the anti-correlation of the two indicators and allows to separate the receivers located in the clay zone (at offsets less than 2200 m) from the ones located in the gravel zone. Receivers in the clay zone show a larger duration (up to 50% more) and a larger negative correlation coefficient between AI and AD than those located in the gravel zone. The increase in AD is an encouraging result in the perspective of reproducing the lengthening of duration observed in the recordings of past events (see e.g. Chaljub, 2017, p. 27-31).

The colored curves in Figure 7a (resp. Figure 7b) represent the spatial variations of AI (resp. AD) for the 10 realizations of the random medium with correlation length  $L_c=200$  m. Compared to the reference model, the average fluctuation of AI (resp. AD) due to the presence of the random heterogeneities is limited to 15 % +/- 7 % (resp. 6 % +/- 3 %) and they seem not to depend on the correlation length (see Figure 9 in the appendix). Such values, although difficult to compare directly, seem consistent with others studies, for example Stripajova et al. (2018) who compare the effects of random heterogeneity on cumulative absolute velocity.

It is likely that the scattering mostly affects surface waves, which have a longer sensitivity and residence time in the heterogeneous area, compared to body waves which have close-to-vertical incidence. The insensitivity to  $L_c$  suggests that the scattering regime is similar for the different random media, most likely dominated by forward, high-frequency ( $k \cdot L_c > 1$ , with  $k$  the wavenumber) scattering of surface waves, which does not dramatically affect AI or AD, unlike the sharp transition between clay and gravel zones which scatters a significant part of surface waves incoming from the Southern edge of the valley. The anti-correlation between AD and AI, and the soil-type dependence of the correlation coefficient, is also unchanged for the case with random heterogeneities, as shown in Figure 8b.

The overall mild effect of the presence of random heterogeneities in the basin on the ground motion indicators presented here can be explained by several factors: (i) the low level of COV used in the simulations, 5%, which is far below values expected from field observations (see Figure 3a for real COV values and see Stripajova et al. (2018) for the effect of raising the COV to 20%); (ii) the fact that density was not perturbed; (iii) the fact that the heterogeneous area is limited to a small (1km x 3 km) zone, which limits the residence time of seismic waves within the random medium in the frequency range considered. The overcoming of those limitations is the object of our immediate perspectives.

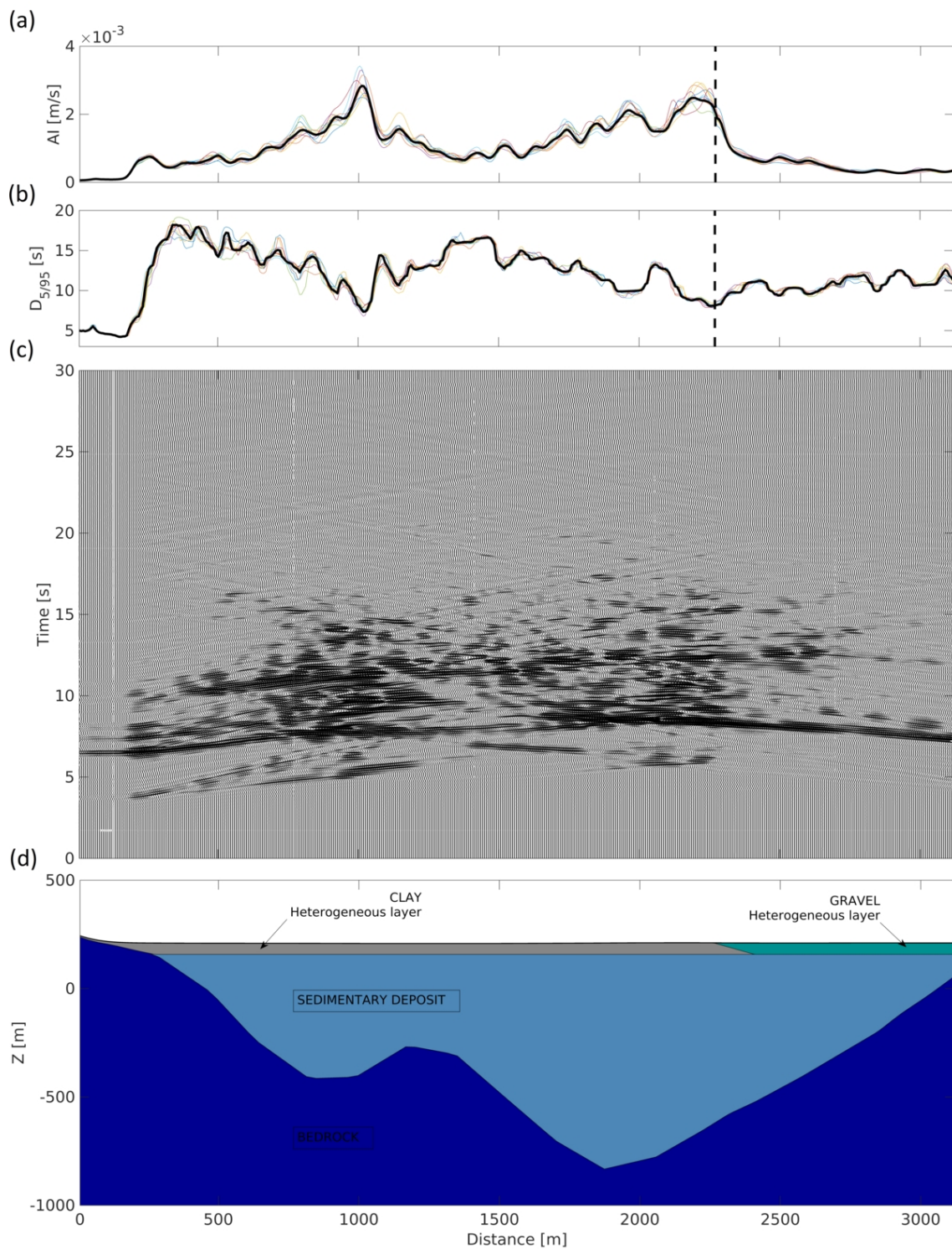


Figure 7: Results obtained along the 2D profile in the ILL area (dashed line in Figure 1a): a) Arias Intensity; b) Trifunac Brady duration; c) East-West component of ground acceleration; d) schematic view of the geological model beneath the profile. The vertical dashed line in a) and b) denotes the location of the clay-gravel transition in the shallow part of the model.

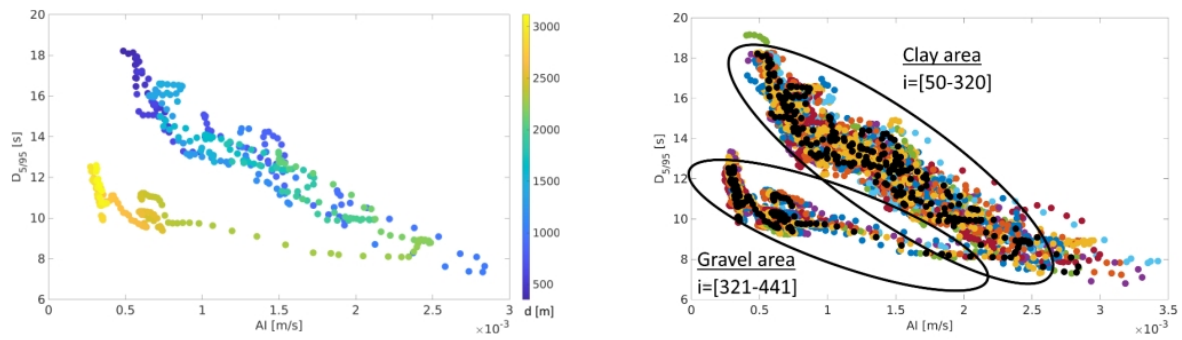


Figure 8: Left: Arias duration plotted as a function of Arias intensity for the background velocity model and receivers located along the profile. Color indicates position along the profile. Right: same for the model having additional random velocity fluctuations with correlation length  $L_c=200$  m. Black dots correspond to the background model and each color corresponds to a different realization of the random medium (10 in total).

## CONCLUSIONS

We presented a methodology to build a realistic velocity model of the Grenoble valley that describes its most heterogeneous shallow part (first 50 – 100 m depth) from a large series of geological, geotechnical and geophysical information accumulated over the years. The model combines a deterministic, geology-driven macro-zoning component and a stochastic description of the small-scale heterogeneity, which allows for numerical simulation of earthquake ground motions at frequencies of interest in engineering applications. The implementation of the stochastic fluctuations in the propagation medium has been verified in a canonical 2D SH configuration by successfully comparing the scattering attenuation measured in the synthetics with theory. Next, we presented preliminary results of the 3D numerical simulation of the seismic response of the Grenoble valley for frequencies up to 5 Hz, in a model comprising a fully heterogeneous area in the Western part of the valley. Our results show a strong effect of the macro-zones on the duration of EGM and a systematic anti-correlation between amplitude and duration for frequencies around 4 – 5 Hz. The influence of random fluctuations is visible on the propagation of diffracted surface waves but is found to be weak in the frequency range considered. Further simulations in more realistic regimes are needed to assess the importance of the small-scale heterogeneity component on EGM, in particular when higher COV, extended heterogeneous macro-zones, density perturbations and possibly higher frequencies are considered.

## ACKNOWLEDGMENTS

This work has been supported by the French National Research Agency (grant N° ANR-17-CE03-0007-03) and by BRGM, ISTERre and EdF internal funds. This work was granted access to the HPC resources of CINES under the allocation 2019-A6 DARI N° A0060410748 attributed by GENCI. MC acknowledges financial support from MINCIENCIAS.

APPENDIX

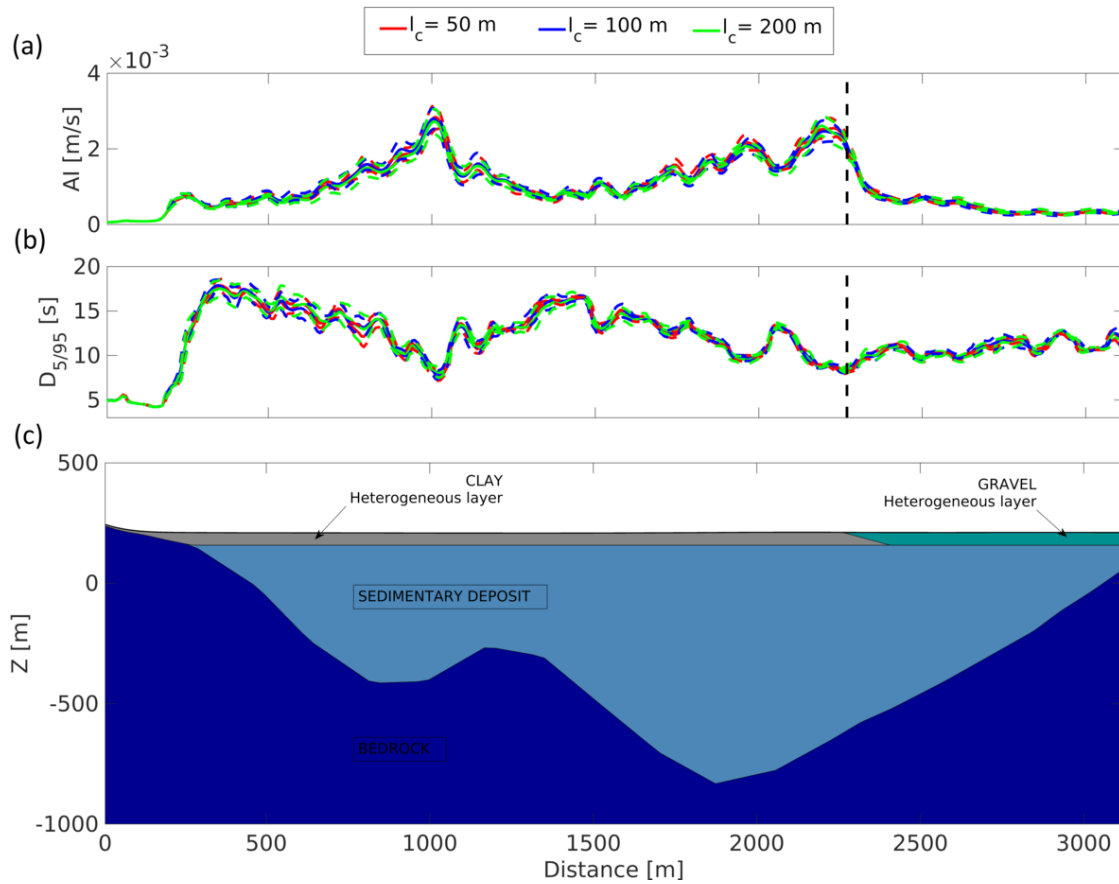


Figure 9: Spatial evolution of a) AI and b) AD along the ILL 2D profile (dashed line in Figure 1a) for three random media with exponential ACF and different correlation lengths:  $L_c=50$  m (red),  $L_c=100$  m (blue) and  $L_c=200$  m (green). The solid curve indicates the mean over 10 realizations, and the dashed lines indicate the mean  $\pm 1$  standard deviation. The geological section below the profile is recalled in c).

## REFERENCES

- Bard, P.-Y., H. Cadet, B. Endrun et al. (2010). "From Non-invasive Site Characterization to Site Amplification: Recent Advances in the Use of Ambient Vibration Measurements", 105–123.
- Capdeville, Y., P. Cupillard & S. Singh (2020). *An introduction to the two-scale homogenization method for seismology*, 217–306, Elsevier.
- Cartier, S. & C. Cornou (2016). *New soil information and financial scenarios to promote earthquake-resistance in the school buildings of Grenoble area*, Octares, Toulouse.
- Chaljub, E. (2017). "Contribution to the numerical estimation of earthquake ground motions", HDR manuscript, Univ. Grenoble Alpes.
- Chaljub, E., P. Moczo, S. Tsuno et al. (2010). "Quantitative Comparison of Four Numerical Predictions of 3D Ground Motion in the Grenoble Valley, France", *Bull. Seismol. Soc. Am.* **100**(4), 1427–1455.
- Chaljub, E., E. Maufroy, P. Moczo et al. (2015). "3-D numerical simulations of earthquake ground motion in sedimentary basins: testing accuracy through stringent models", *Geophys. J. Int.* **201**(1), 90–111.
- Collombet M. (2009). "Notice explicative pour la mise en place d'un SIG à partir de données de forages géotechniques", Tech. Report, Projet RDT-SIRSEG, Université Joseph Fourier, 22 p., in french.
- Cornou, C. (2002). "Traitement d'antenne et imagerie sismique dans l'agglomération grenobloise (Alpes françaises) : implications pour les effets de site", PhD thesis, (260 p.), Univ. J. Fourier, Grenoble.
- De Carvalho Paludo, L., V. Bouvier & R. Cottureau (2018). "Scalable parallel scheme for sampling of Gaussian random fields over very large domains", *Int. J. Numer. Methods Eng.* **117**(8), 845–859.
- De Martin, F. (2011). "Verification of a Spectral-Element Method Code for the Southern California Earthquake Center LOH.3 Viscoelastic Case", *Bull. Seismol. Soc. Am.* **101**(6), 2855–2865.
- Emoto, K. & Sato, H. (2018). "Statistical characteristics of scattered waves in three-dimensional random media: comparison of the finite difference simulation and statistical methods", *Geophys. J. Int.*, **215**, 585-599
- Garofalo, F., S. Foti, F. Hollender et al. (2016). "InterPACIFIC project: Comparison of invasive and non-invasive methods for seismic site characterization. Part II: Inter-comparison between surface-wave and borehole methods", *Soil Dyn. Earthquake Eng.* **82**241–254.
- Ghanem, R., G. & P. D. Spanos (1991). *Stochastic Finite Elements: A Spectral Approach*, Springer New York.
- Grandjean, J. (2013). "Imaging superficial structures in the Grenoble basin through the correlation of geophysical and geotechnical data.", master report, Univ. J. Fourier, Grenoble.
- Guéguen, P., C. Cornou, S. Garambois et al. (2007). "On the Limitation of the H/V Spectral Ratio Using Seismic Noise as an Exploration Tool: Application to the Grenoble Valley (France), a Small Aspect Ratio Basin", *Pure Appl. Geophys.* **164**(1), 115–134.
- Hartzell, S., Harmsen, S. & Frankel, A. (2010). "Effects of 3D Random Correlated Velocity Perturbations on Predicted Ground Motions", *Bull. Seismol. Soc. Am.*, **100**, 1415-1426.
- Hollender, F., C. Cornou, A. Dechamp et al. (2017). "Characterization of site conditions (soil class, VS30, velocity profiles) for 33 stations from the French permanent accelerometric network (RAP) using surface-wave methods", *Bull. Earthquake Eng.* **16**(6), 2337–2365.
- Imperatori, W. & Mai, P. M. (2012). "Broad-band near-field ground motion simulations in 3-dimensional scattering media", *Geophys. J. Int.*, **192**, 725-744.
- Iwaki, A., Maeda, T., Morikawa, N. et al. (2018). "Effects of random 3D upper crustal heterogeneity on long-period ( $\geq 1$  s) ground-motion simulations". *Earth Planets Space* **70**, 156.
- Karhunen, K. (1947). "*Über lineare Methoden in der Wahrscheinlichkeitsrechnung*", Universität Helsinki.
- Komatitsch, D. & J.-P. Vilotte (1998). "The spectral element method: An efficient tool to simulate the seismic response of 2D and 3D geological structures", *Bull. Seismol. Soc. Am.* **88**(2), 368-392.
- Lacroix, B. (1971). "Contribution a l'étude hydrogéologique de la plaine de Grenoble", Grenoble, 3<sup>rd</sup> cycle thesis; 1971, 125 p., Univ. J. Fourier, Grenoble.
- Lebrun, B., D. Hatzfeld & P.-Y. Bard (2002). "Site Effect Study in Urban Area: Experimental Results in Grenoble (France)", 2543–2557, *Earthquake Microzoning*, Birkhäuser Basel.

- Liu, Y., J. Li, S. Sun et al. (2019). "Advances in Gaussian random field generation: a review", *Comput. Geosci.* **23**(5), 1011–1047.
- Maufroy, E., E. Chaljub, N. P. Theodoulidis et al. (2017). "Source-Related Variability of Site Response in the Mygdonian Basin (Greece) from Accelerometric Recordings and 3D Numerical Simulations", *Bull. Seismol. Soc. Am.* **107**(2), 787–808.
- Panunzio, A. M., R. Cottureau & G. Puel (2018). "Large scale random fields generation using localized KarhunenLoève expansion", *Adv. Model. Simul. Eng. Sci.* **5**(1).
- Pitarka, A. & R. Mellors (2021). "Using Dense Array Waveform Correlations to Build a Velocity Model with Stochastic Variability", *Bull. Seismol. Soc. Am.*
- Przybilla, J., Korn, M. & Wegler, U. (2006). "Radiative transfer of elastic waves versus finite difference simulations in two-dimensional random media", *J. Geophys. Res.*, **111**.
- Rivanedeira, F. (2012). "Imaging of Grenoble sub-surface structure by integration of geological and geophysical data.", master thesis, Univ. J. Fourier, Grenoble.
- Sato, H., M. C. Fehler & T. Maeda (2012). *Seismic Wave Propagation and Scattering in the Heterogeneous Earth: 2nd Edition*, Springer Berlin Heidelberg.
- Scalise, M., A. Pitarka, J. N. Louie et al. (2020). "Effect of Random 3D Correlated Velocity Perturbations on Numerical Modeling of Ground Motion from the Source Physics Experiment", *Bull. Seismol. Soc. Am.* **111**(1), 139–156.
- Søndergaard, J., Lophaven, S. & Nielsen, H.B., 2002. DACE: A Matlab Kriging Toolbox. *Mathematical Modelling*, (September).
- Stripajova, S., P. Moczo, J. Kristek et al. (2018). "Extensive numerical study on identification of key structural parameters responsible for site effects", 16th European Conference on Earthquake Engineering, Thessaloniki, Greece.
- Tadenuma, S. (2003). "Etude des formations superficielles du bassin grenoblois.", Tech. Report, Polytech Grenoble, in french.
- Thouvenot, F., J. Fréchet, L. Jenatton et al. (2003). "The Belledonne Border Fault: identification of an active seismic strike-slip fault in the western Alps", *Geophys. J. Int.* **155**(1), 174–192.
- Tsuno, S., C. Cornou & P.-Y. Bard (2008). "Superficial S-wave velocity and damping factor model determined by the MASW measurement in the Grenoble sedimentary basin", 14th World Conference on Earthquake Engineering, Beijing, China.
- Vallon, M. (2014). "Estimation de l'épaisseur d'alluvions quaternaires dans la cuvette grenobloise par inversion des anomalies gravimétriques.", Tech. Report, Univ. J. Fourier, in french.
- Trifunac, M. D. & A. G. Brady (1975). "A study on the duration of strong earthquake ground motion", *Bull. Seismol. Soc. Am.* **65**(3), 581-626.
- Withers, K. B., Olsen, K. B., Day, S. M. et al. (2018). "Ground Motion and Intraevent Variability from 3D Deterministic Broadband (0–7.5 Hz) Simulations along a Nonplanar Strike-Slip Fault", *Bull. Seismol. Soc. Am.*, **109**, 229-250.